



Full Length Article

# Effective femtosecond laser shock peening on a Mg–3Gd alloy at low pulse energy 430 $\mu\text{J}$ of 1 kHz

Chenghao Lu<sup>a</sup>, Licheng Ge<sup>a</sup>, Bing Zhu<sup>a</sup>, Yangxin Li<sup>b</sup>, Xianfeng Chen<sup>a</sup>, Xiaoqin Zeng<sup>b</sup>, Yuping Chen<sup>a,\*</sup>

<sup>a</sup>State Key Laboratory of Advanced Optical Communication Systems and Networks, Department of Physics and Astronomy, Shanghai Jiao Tong University, Shanghai 200240, PR China

<sup>b</sup>National Engineering Research Center of Light Alloy Net Forming and State Key Laboratory of Metal Matrix Composite, Shanghai Jiao Tong University, Shanghai 200240, PR China

Received 11 March 2019; received in revised form 20 May 2019; accepted 20 May 2019  
Available online 29 June 2019

## Abstract

In this paper, microstructure evolution and hardness of Mg–3Gd alloy treated by femtosecond (fs) laser shock peening (LSP) with direct and confined ablation modes were investigated in detail. Under a relatively low pulse energy of 430  $\mu\text{J}$  with a repetition of 1 kHz, the surface hardness of sample has been enhanced by 70% effectively. Compared with ns-LSP with pulse fluence of 71.7 J/cm<sup>2</sup>, fs-LSP with pulse fluence of 34.2 J/cm<sup>2</sup> is superior in the hardness increment, both of which are in the same order of magnitude. A distinct grain refinement of surface layer has been discovered and results in the increase of hardness. Nonuse of absorption and confining layers and the employment of the industry commercial fs laser with high repetition can inspire big potential LSP application in special metal material.

© 2019 Published by Elsevier B.V. on behalf of Chongqing University.

This is an open access article under the CC BY-NC-ND license. (<http://creativecommons.org/licenses/by-nc-nd/4.0/>)

Peer review under responsibility of Chongqing University

**Keywords:** Laser shock peening; Femtosecond laser; Mg–3Gd alloy hardness; Surface treatment.

## 1. Introduction

Magnesium alloys have been a desirable candidate as important structural materials for weight saving in the automotive and aerospace industries [1,2]. However, the disadvantages of low strength and poor formability limited their applications. Conventional strengthening methods for magnesium alloys include shot peening, hammer peening, surface mechanical attrition treatment [3,4], surface rolling and high-speed machining.

As a new surface modification technology of materials, laser shock peening (LSP) has been applied on metals like steels [5], Ti alloys [6] and Al alloys [7] due to its high efficiency, simple operability, reliability and comprehensive performance. After being heated by an intense ultrashort laser

(intensity up to 1 GW/cm<sup>2</sup>), the solid material rapidly transforms into a plasma state accompanied by volume expansion. In the process of expansion [8,9], shock waves propagate in the solid interior in the form of mechanical waves. When the magnitude of shock wave exceeds the dynamic yield strength, high density dislocation arrays can be formed, which can help improve the yield strength and hardness of laser peened specimens [10–12].

The physical mechanism and applications of nanosecond laser shock peening have been studied theoretically and experimentally. A typical nanosecond laser system has a single pulse energy of 10–100 J with 10–100 ns pulse duration and 5–10 Hz repetition. Fabbro et al. [13], compared the difference of laser induced pressure under “direct ablation” mode and the “confined ablation” mode in ns-LSP and found that the generated pressure in confined ablation mode is 4–10 times greater than that in direct ablation mode. Since then, subsequent experiments on ns-LSP basically adopted the confined mode.

\* Corresponding author.

E-mail address: [ypchen@sjtu.edu.cn](mailto:ypchen@sjtu.edu.cn) (Y. Chen).

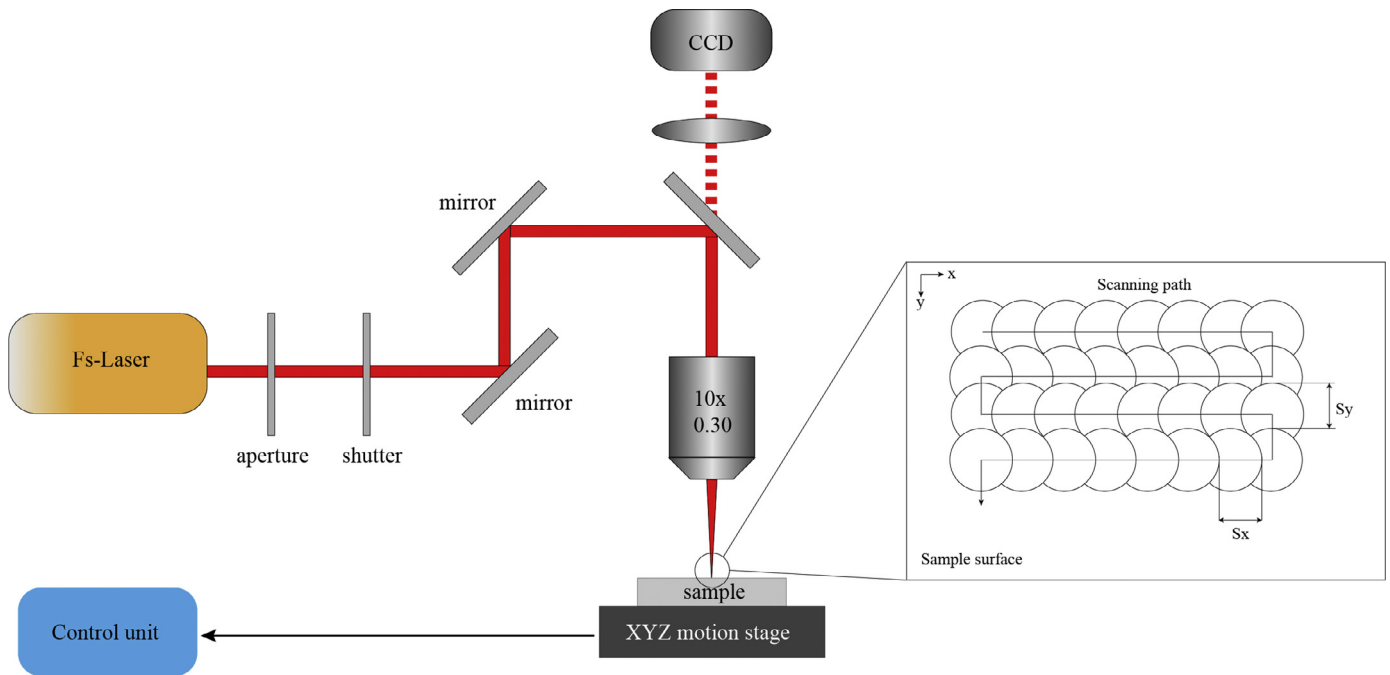


Fig. 1. Schematic setup. Left is the LSP experimental setup and right is the scanning path of the laser pulses.

One of the main disadvantages of ns-LSP is the reliability problem of high pulse energy and a very low repetition.

Later, with the further development of laser technology, femtosecond laser has been applied to LSP. The pulse width and single pulse energy of femtosecond laser are much smaller than that of nanosecond laser. The extremely short pulse width of femtosecond laser results in extremely high peak power (intensity can exceed  $10\text{TW}/\text{cm}^2$ ), which means that a lower laser power can generate a higher shock wave on the surface of the material [14]. When it comes to fs-LSP, some groups have controversy about whether to use the “direct ablation” mode or the “confined ablation” mode. Nakano et al. [15]. first demonstrated the fs-LSP on SUS304 stainless steel in water and Sano et al. [16]. performed fs-LSP on a 2024 aluminum alloy without any sacrificial overlays, both of which indicated the dramatic improvement of surface properties. While Lee and Kannatey-Asibu [17] investigated the feasibility of fs-LSP with a zinc coating in water to find out that the hardness was not significantly enhanced.

In this paper, a direct ablation group and three confined ablation groups are set up. Results show that direct ablation mode can improve the surface hardness most significantly. Under a relatively low single pulse energy of  $430\ \mu\text{J}$  with  $1\ \text{kHz}$ , the surface hardness of sample has been enhanced by 70%, which is superior to a hardness of 45.1% increment induced by a nanosecond LSP with pulse energy of  $9\ \text{J}$ . It is noted that the fs-LSP is superior to ns-LSP in the hardness increment at the same order single pulse fluence of  $34.2$  and  $71.7\ \text{J}/\text{cm}^2$ . However, the former was performed by the fs laser at low single pulse energy and high repetition.

## 2. Experimental setup

The selected sample was a nominal as-cast Mg–3Gd (wt%) alloy. After casting, the sample was homogenized and annealed for 2 h at  $500\ ^\circ\text{C}$ . Then the sample was cut into a rectangular plate of  $30 \times 20 \times 5\ \text{mm}$ , and the surface was polished, scrubbed with alcohol. Finally, it was cleaned with ultrasonic wave.

A commercial Ytterbium-doped femtosecond laser system is used in the experiments. The pulse duration is  $600\ \text{fs}$  at a nominal wavelength of  $1030\ \text{nm}$ , with a repetition rate of  $1\ \text{kHz}$ . The power of laser system can be adjusted up to  $430\ \text{mW}$ , which means a single pulse energy is  $430\ \mu\text{J}$ . The numerical aperture of the objective is  $0.3$ , the focal spot diameter is about  $40\ \mu\text{m}$ . The laser intensity ( $I$ ) and laser fluence ( $F$ ) are given by Eqs. (1) and (2), respectively.

$$I = \frac{4E}{\pi\tau D^2} \quad (1)$$

$$F = \frac{4E}{\pi D^2} \quad (2)$$

where  $E$  represents single laser pulse energy,  $\tau$  and  $D$  are the pulse duration and diameter of focal spot. The corresponding peak intensity and fluence can be  $57.1\ \text{TW}/\text{cm}^2$  and  $34.2\ \text{J}/\text{cm}^2$ .

The left of Fig. 1 shows the experimental setup of LSP. The femtosecond laser passes through a semi-transparent and semi-reflective mirror, part of the beam is focused on the sample surface through the objective lens, and the other part of the beam enters the CCD to monitor the surface structure.

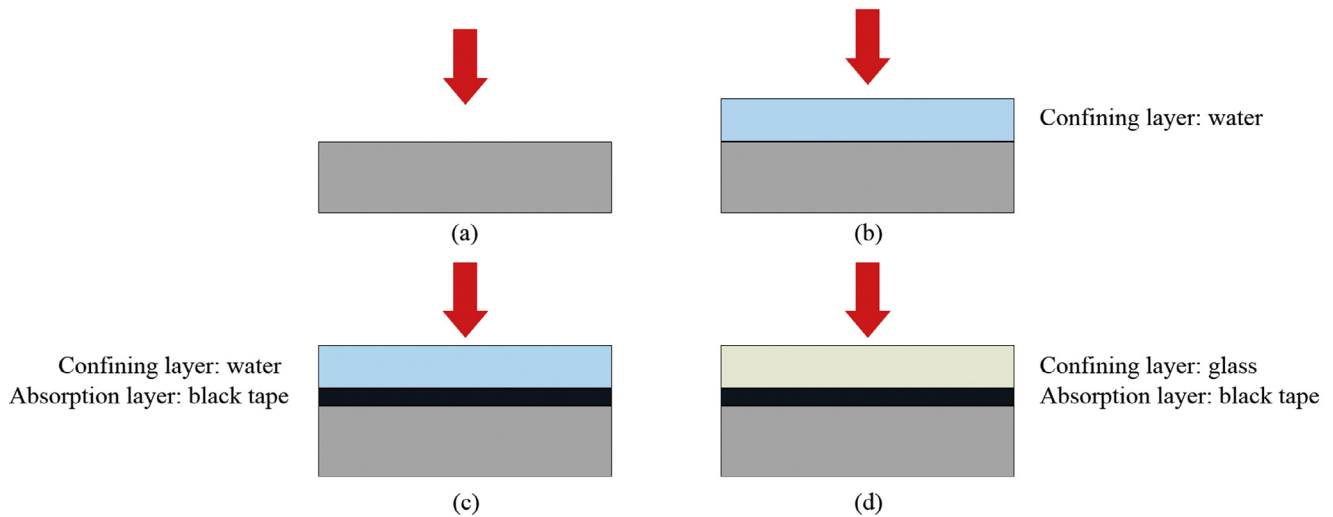


Fig. 2. Four different LSP treatments on the Mg-3Gd alloy. (a) direct LSP in air, (b) LSP in water, (c) LSP with a black tape in water and (d) LSP with a black tape under a glass overlay.

The sample is placed on a three-dimensional translation platform operated by the control center. The scanning path of the laser is shown on the right of Fig. 1. The coverage is defined as the overlap ratio between adjacent focal spot

$$\eta_i = 1 - \frac{S_i}{2R} \times 100\% \quad (i = x \text{ or } y) \quad (3)$$

where  $R$  represents the radius of the focal spot,  $S_i$  represents the distance between the adjacent focal spot in horizontal ( $x$ ) or vertical ( $y$ ) direction.

In this paper, a direct ablation group (a) and three confined ablation groups (b–d) are set up as illustrated by Fig. 2. Group (a) is directly impacted by femtosecond laser pulses without any absorption layer in air. The other three confined ablation groups are designed based on whether the absorption layer is included and different materials of the absorption layer and the confining layer. Group (b) is added a confining layer (water), group (c) is added an absorption layer (black tape) and a confining layer (water), group (d) is the same as group (c), but the material of the absorption layer and the confining layer is replaced by black tape and glass. The thickness of water layer, black tape and glass is 2 mm, 150  $\mu\text{m}$  and 1 mm respectively. Black tape is 3M electrical insulation tape 1600, the main component is polyvinyl chloride (PVC). All experiments were treated by the fs-laser of 1 kHz with a coverage  $\eta_x = \eta_y = 80\%$ .

### 3. Results and discussion

The hardness values of Mg-3Gd alloys by four different LSP treatments are evaluated by Vickers hardness test, where the force is 50N and the loading time is 10s. In the control experiment, each experimental group used a sample independently. Five samples were used in four experimental groups and one blank group. These samples were cut from the same large sample. The Vickers micro-hardness measurement data

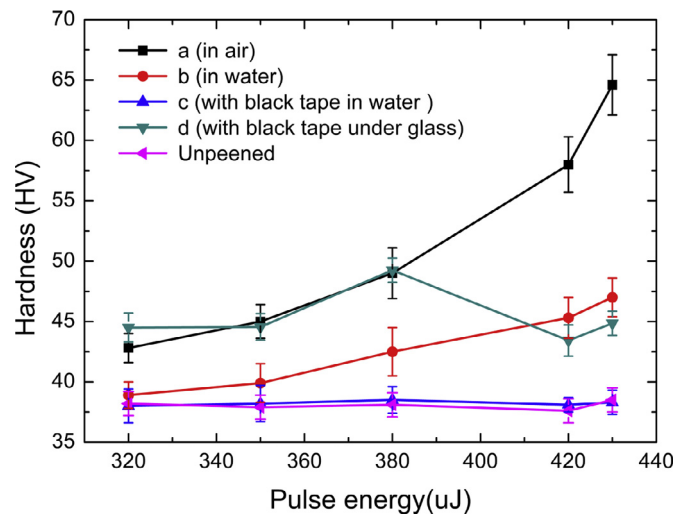


Fig. 3. Hardness distribution with pulse energy under four different overlays and a blank group. The black line represents group (a) which is direct peened in air. The red line is LSP with a water overlay. The blue one is LSP with black tape in water. The green one is LSP with black tape under glass. The purple one is the original surface without LSP. All experiments were treated by the fs-laser of 1 kHz with a coverage of 80%.

of the sample surfaces under four treatments is summarized in Fig. 3.

As shown in Fig. 3, the hardness values of Mg-3Gd alloy after different LSP treatments are all larger than the unpeened material. The average hardness of Mg-3Gd alloy before LSP treatment is  $38 \pm \text{HV}$ . The Vickers hardness increases with the increase of laser pulse energy in group (a) and (b). With a pulse energy of 430  $\mu\text{J}$ , the surface hardness of (a) and (b) are  $64.6 \pm \text{HV}$  and  $47 \pm \text{HV}$ , which means the hardness is increased by 70% in air, but only 23.7% in water, indicating that the existence of the confining layer reduces the hardening effect. The results of group (c) showed no significant change compared with the untreated samples. When

Table 1  
Comparison of typical reported hardness increments for different LSP parameters. The increment of this study is also listed.

Material	Pulse duration	Wavelength	Single pulse energy	Frequency	LSP mode	Hardness increment (%)	Source
TC17 titanium alloy	20ns	1064 nm	5 J	1 Hz	Al foil as absorption layer in water	21	[6]
Al-6061-T6 alloy	8 ns	1064 nm	1.2 J	10 Hz	In water	20.5	[7]
SUS304	191 fs	800 nm	300 $\mu$ J	100 Hz	In water	104.4	[15]
low-carbon steel	200 fs	775 nm	643.7 $\mu$ J	1 kHz	With Zinc coating in water	9.3	[17]
Al-2024-T351 alloy	120 fs	800 nm	600 $\mu$ J	Unmentioned	In air	35.3	[16]
Mg-3Gd alloy	15 ns	1064 nm	9J (71.7J/cm <sup>2</sup> )	5 Hz	Black tape as absorption in air	45.1	Our work
Mg-3Gd alloy	600 fs	1030 nm	430 $\mu$ J (34.2J/cm <sup>2</sup> )	1 kHz	In air	70	Our work

the laser focuses on the absorption layer to produce plasma shock wave, it causes severe oscillation of the water surface and generates many water bubbles, which result in the following laser pulses scattered by the water surface and bubbles, and the other part cannot be well focused on the absorption layer. When the plasma wave cannot be produced continuously, which makes the hardening effect worse. The Vickers hardness values of group (d) increase with pulse energy when pulse energy is smaller than 380  $\mu$ J, then begin to decrease, and then begin to increase again when pulse energy is over 420  $\mu$ J. This phenomenon is probably related to the thickness of the black tape. When the single pulse energy is less than 380  $\mu$ J, the tape is not ablated through, so the shock wave increases with the increase of pulse energy. But when the single pulse reaches 420  $\mu$ J, the single pulse energy is almost enough to burn through the tape, where the result of group (d) is equivalent to directly impacting the sample in the air, similar to that of group (a). Under this condition, part of the pulse energy is used to burn through the tape and the other part acts on the surface. As a result, the hardness value decreased compared with that of 380  $\mu$ J. When the pulse energy exceeds 420  $\mu$ J, the laser pulse directly impacts the surface of the sample and the hardness begin to rise.

In order to better explain the phenomenon that the strengthening effect of the direct LSP group (a) is better than that of the confined LSP groups (b–d), we use two physical models to quantitatively analyze the plasma wave pressure produced by femtosecond laser in these two modes. For the direct LSP group, Phipps et al. [18] group's model was applied. For a constant absorbed laser intensity  $I$ , wavelength  $\lambda$  and a laser pulse duration  $\tau$ , the peak pressure  $P$  are given by the empirical trend

$$P(\text{GPa}) = bI(I\lambda\sqrt{\tau})^n \quad (4)$$

where coefficient  $b$  is material dependent and  $n = -0.3 \pm 0.03$  is the same for C–H material or the aluminum alloys. Here, we take  $b = 5.6$  and  $n = -0.3$ . For the confined LSP groups, Fabbro et al. [13] group's model was applied. The peak pressure  $P$  are given by

$$P(\text{GPa}) = 0.01 \sqrt{\frac{\alpha}{2\alpha + 3}} \sqrt{Z(\text{g cm}^{-2}\text{s}^{-1})I(\text{GW/cm}^2)} \quad (5)$$

where  $\alpha$  with a typical value of 0.1 is the fraction of the internal energy devoted to the thermal energy of laser induced

plasma,  $Z$  is a reduced acoustic impedance of the confining  $Z_1$  and target  $Z_2$  materials given by

$$\frac{2}{Z} = \frac{1}{Z_1} + \frac{1}{Z_2} \quad (6)$$

In this paper, a 600 fs laser pulse with a nominal wavelength of 1030nm was used. The laser intensity is 57.1 TW/cm<sup>2</sup> and  $Z = 2.1 \times 10^6 \text{g}/(\text{cm}^2 \text{s})$  for the water/magnesium alloy interface, then we can calculate the peak pressure of direct LSP and confined LSP mode is 3608 GPa and 612 GPa, respectively. The peak pressure of the direct LSP mode is about 6 times that of the confined LSP mode. Although the above calculations are not particularly accurate, the difference in the magnitude of pressure is sufficient to quantify that direct LSP can obtain higher and stronger shock waves.

A comparison of some typical reported hardness increments for different LSP parameters is listed in Table 1. The first four groups in the table are ns-LSP experiments and the last four groups are fs-LSP experiments. By comparison, it is obvious that the single pulse energy used in fs-LSP experiment is far less than that in ns-LSP experiment, but fs-LSP has greater advantages for improving hardness. Moreover, for ns-LSP, the use of confined ablation mode can improve enhancement, but for fs-LSP, direct ablation mode has greater advantages. Generally speaking, fs-LSP requires less single pulse energy than ns-LSP, together with a simpler experimental setup. It's worth being mentioned that a similar ns-LSP is also carried out on the Mg–3Gd alloy. With a maximum pulse energy of 9J at the focal diameter of 4 mm, the hardness can be increased by 45.1%. It is noted that the fs-LSP is superior to ns-LSP in the hardness increment at the same order single pulse fluence of 34.2 and 71.7J/cm<sup>2</sup>.

According to the Fig. 3, the best hardening effect can be achieved under the direct LSP mode. Therefore, under this mode, further investigation of the influence of two parameters pulse energy and coverage on hardness enhancement was demonstrated. As shown in Fig. 4, the left group is treated with direct LSP in air under the 80% coverage and 1kHz fs-laser. The right group is treated with direct LSP under the 200  $\mu$ J and 1kHz fs-laser. The hardness of sample surface increases linearly with pulse energy and coverage respectively, which indicates that a better strengthening effect can be achieved by increasing both pulse energy and coverage. The fs-laser space distribution of energy can be described by

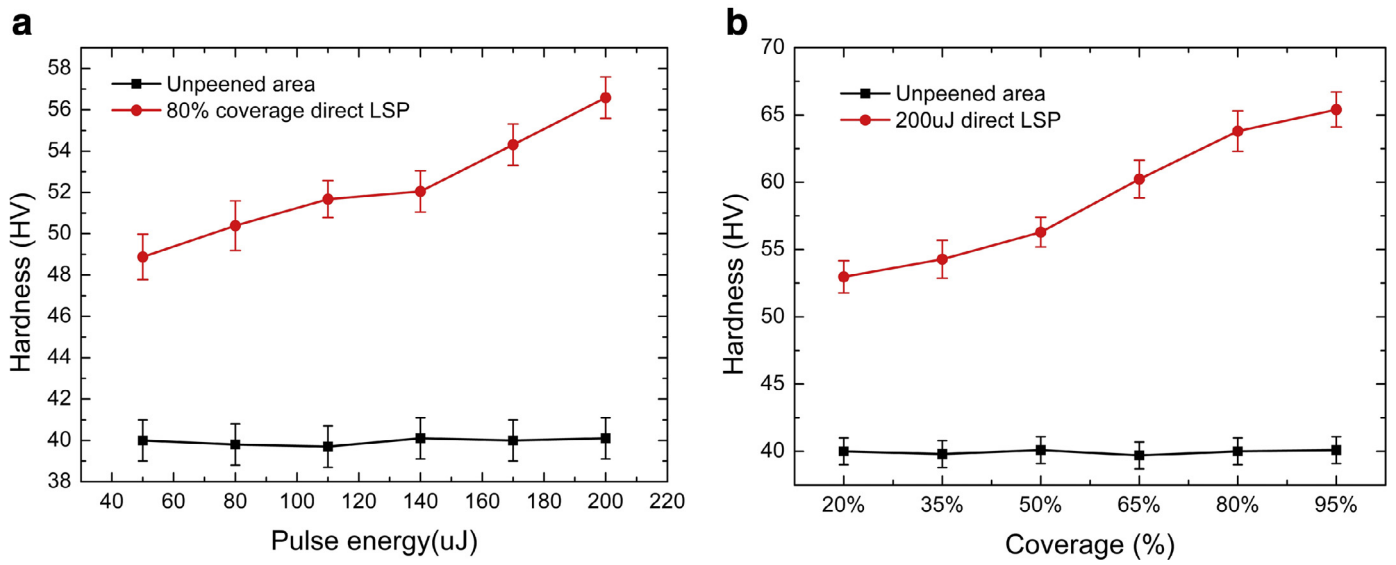


Fig. 4. Hardness distribution with different pulse energy and coverage. (a) direct LSP in air under the 80% coverage and 1 kHz fs-laser. (b) direct LSP under the 200 μJ and 1 kHz fs-laser.

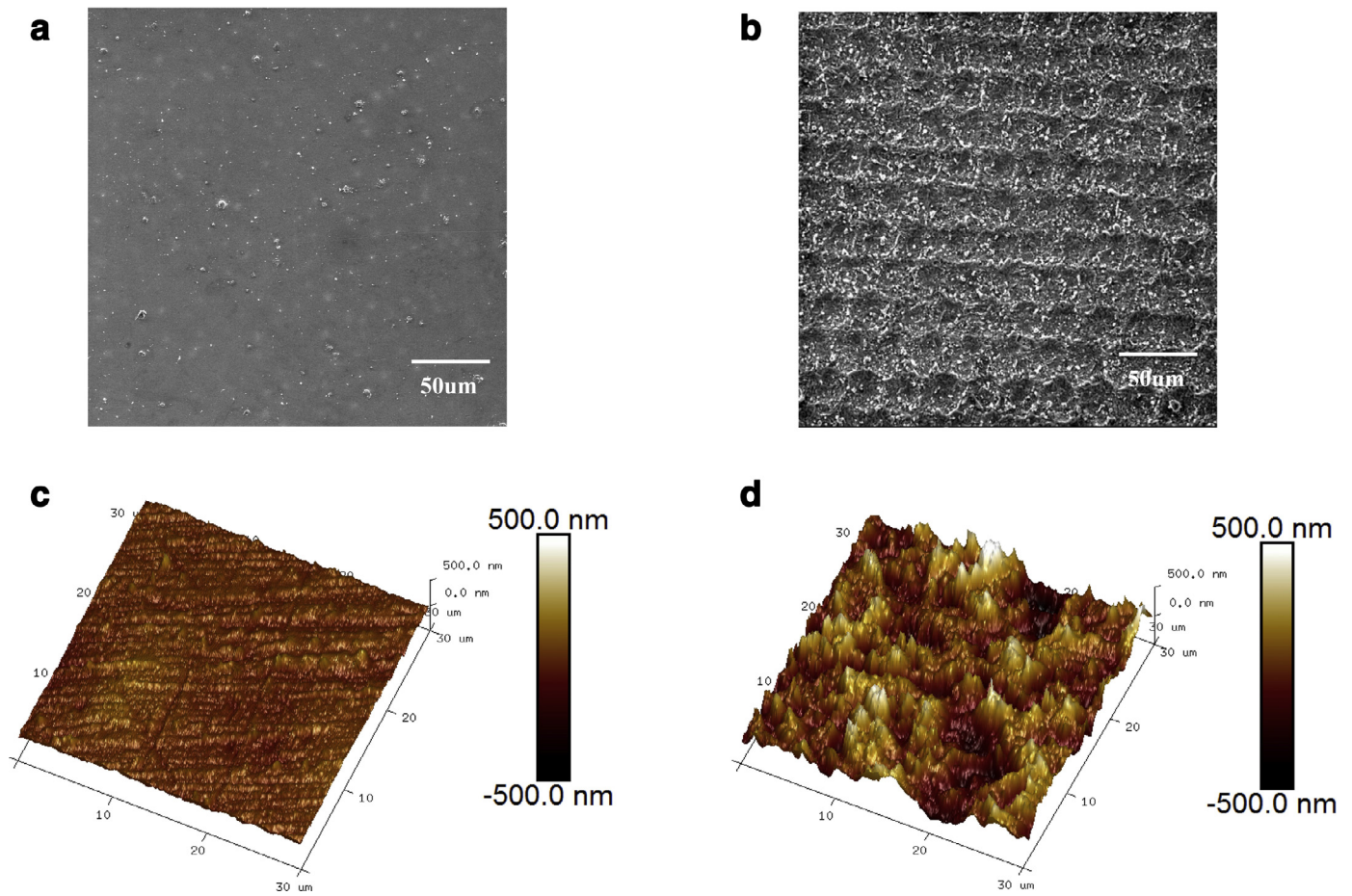


Fig. 5. SEM and AFM surface morphology. (a) and (b) are SEM surface morphology of unpeened and LSP treated (with 80% coverage and 200 μJ fs-laser) areas. (c) and (d) are the corresponding AFM pictures of (a) and (b), respectively.

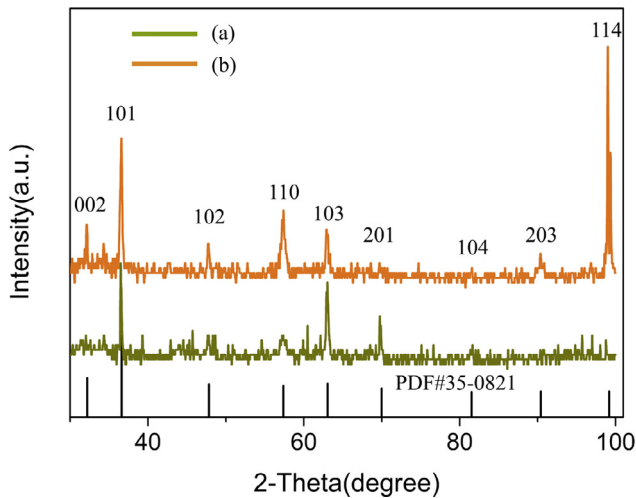


Fig. 6. XRD analysis of sample surfaces. (a) Unpeened sample. (b) Treated by direct LSP with 80% coverage and 200  $\mu\text{J}$  fs-laser.

Gaussian profile. When coverage increases, the adjacent focal spots are closer to each other, increasing the local power density dramatically to induce higher pressure. The hardness increase with the increase of pulse energy can be understood easily, more power density can induce higher pressure. Because the maximum pulse energy of the laser is 430  $\mu\text{J}$ , it is not clear whether the hardness continues to grow when pulse energy is far beyond 430  $\mu\text{J}$ .

Two samples are selected for further analysis by scanning electron microscope (SEM) and atomic force microscopy (AFM). Fig. 5(a) and (b) is SEM surface morphology of

unpeened and LSP treated areas. Fig. 5(c) and (d) is the corresponding AFM pictures of the mentioned two areas. The surface of unpeened sample appear smooth and flat. There are some small particles on the surface. Fig. 5(b) is the area treated by direct LSP with 80% coverage and 200  $\mu\text{J}$  fs-laser. The surface is ablated apparently. There are a lot of dents and microstructures on the surface. After LSP, the surface of the sample is heated and transformed into plasma, along with the shock, vaporization, melting, resolidation etc. The wave pressure once exceeds the dynamic yield strength and surface will undergo permanent deformation. The formation of each dent includes both the ablation-induced material removal and the impact of the shock wave. From Fig. 5(c) and (d), it is evident that the LSP treated area shows higher surface roughness than that of unpeened area.

The X-ray diffraction of angle range 30–100° was presented in Fig. 6. The green line represents the unpeened sample and the orange line represents the sample treated by direct LSP with 80% coverage and 200  $\mu\text{J}$  fs-laser. The peaks of 101, 110 and 203 become broader, indicating that there exists grain refinement after LSP. The optical micrograph (OM) and scanning electron microscope (SEM) images of sample cross section are shown in Fig. 7. The OM image of polished untreated surface appears relatively smooth and the LSP surface exhibits appreciable roughness, as illustrated in Fig. 7(a). In order to verify the near surface changes before and after the LSP treatment, three SEM images are presented in Fig. 7(b)–(d). Compared with Fig. 7(b), the valleys induced by ablative interaction and shock wave pressure on the surface can be observed on the top surface. This confirms that surface melting due to direct laser interaction does not have

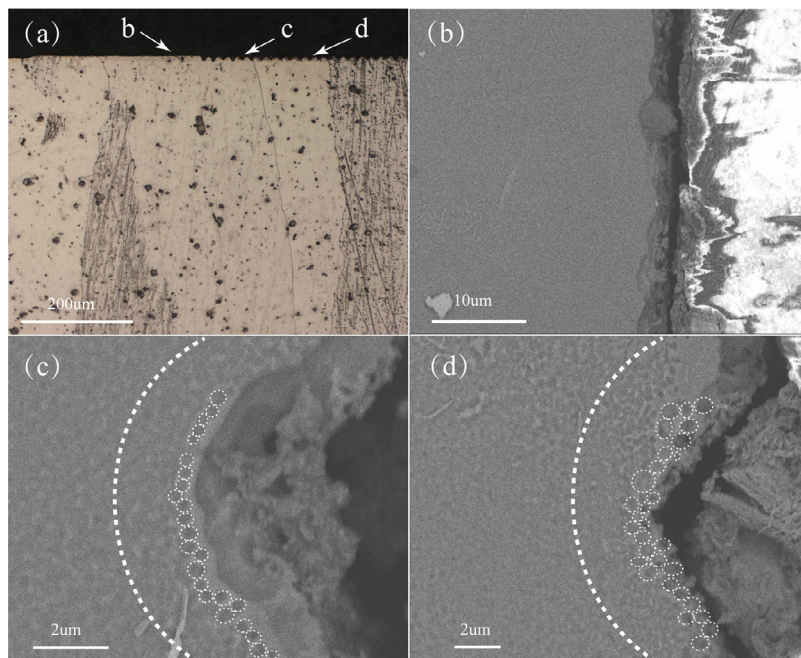


Fig. 7. (a) Optical micrograph of sample cross section, surface with straight line is untreated surface and surface with a zigzag is treated area by LSP with 80% coverage and 200  $\mu\text{J}$  fs-laser. (b)–(d) are SEM images corresponding to the marked places in (a). Grain refinement layer (area marked by the dashed line) can be discovered in (c) and (d).

any appreciable effect beyond a depth of few micrometers from the top surface. Also, a grain refinement thin layer of about 2–4  $\mu\text{m}$  can be observed in Fig. 7(c) and (d). The original grain size of Mg–3Gd is about 200  $\mu\text{m}$ , whereas the grain size of surface layer is decreased to 521.7 nm with a standard deviation of 175.9 after LSP treatment. This confirms that the hardness increase can be attributed to the surface grain refinement.

#### 4. Conclusions

In this paper, the effect of femtosecond laser shock under different processing conditions is investigated. It is found that the effect of direct LSP mode is more remarkable than that of confined LSP mode. Although the direct laser peening is based on sacrificing the surface layer of the sample, this method can dramatically improve the hardness with high efficiency. Under the direct LSP of 430  $\mu\text{J}$  pulse energy, the surface hardness of the sample can be increased by 70%. Compared with the hardness increment induced by ns-LSP, fs-LSP requires relatively low average power and can have better performance in the hardening effect. In addition, a better strengthening effect can be achieved by increasing laser pulse energy and coverage. The physical mechanism of hardening effect is also discussed. OM, SEM, AFM and XRD pictures indicate that the laser induced shock results in many microstructures, high roughness and grain refinement of the sample surface, which could contribute to the increase of hardness.

The fs-LSP technology may have a great potential to be applied in various fields where conventional peening methods cannot be used. For example, direct LSP can improve the efficiency by using the industry commercial laser and without preparation of the absorption layer or the confining layer.

#### Declarations of interest

None.

#### Acknowledgments

The authors thank Professor Yongxiang Hu for the ns-LSP experiment on Mg–3Gd alloy and his useful discussion. The

research was supported by the National Key R&D Program of China (2017YFA0303700); the National Natural Science Foundation of China (NSFC) (11574208).

#### References

- [1] P. Ji, R. Long, L. Hou, R. Wu, J. Zhang, M. Zhang, *Surf. Coat. Technol.* 350 (2018) 428–435, doi:[10.1016/j.surfcoat.2018.07.038](https://doi.org/10.1016/j.surfcoat.2018.07.038).
- [2] R.Z. Wu, Y.D. Yan, G.X. Wang, L.E. Murr, W. Han, Z.W. Zhang, M.L. Zhang, *Int. Mater. Rev.* 60 (2015) 65–100, doi:[10.1179/1743280414Y.0000000044](https://doi.org/10.1179/1743280414Y.0000000044).
- [3] K. Lu, J. Lu, *Mater. Sci. Eng. A* 375 (2004) 38–45, doi:[10.1016/j.msea.2003.10.261](https://doi.org/10.1016/j.msea.2003.10.261).
- [4] X.Y. Shi, Y. Liu, D.J. Li, B. Chen, X.Q. Zeng, J. Lu, W.J. Ding, *Mater. Sci. Eng. A* 630 (2015) 146–154, doi:[10.1016/j.msea.2015.02.009](https://doi.org/10.1016/j.msea.2015.02.009).
- [5] D. Lee, E. Kannatey-Asibu Jr, *J. Laser Appl.* 23 (2011) 022004, doi:[10.2351/1.3573370](https://doi.org/10.2351/1.3573370).
- [6] X. Nie, W. He, Q. Li, N. Long, Y. Chai, *J. Laser Appl.* 25 (2013) 042001, doi:[10.2351/1.4800444](https://doi.org/10.2351/1.4800444).
- [7] A. Salimianrizi, E. Foroozmehr, M. Badrossamay, H. Farrokhpour, *Opt. Lasers Eng.* 77 (2016) 112–117, doi:[10.1016/j.optlaseng.2015.08.001](https://doi.org/10.1016/j.optlaseng.2015.08.001).
- [8] B.P. Fairand, A.H. Clauer, *J. Appl. Phys.* 50 (1979) 1497–1502, doi:[10.1063/1.326137](https://doi.org/10.1063/1.326137).
- [9] R. Fabbro, P. Peyre, L. Berthe, X. Scherpereel, *J. Laser Appl.* 10 (1998) 265–279, doi:[10.2351/1.521861](https://doi.org/10.2351/1.521861).
- [10] Y. Sano, M. Obata, T. Kubo, N. Mukai, M. Yoda, K. Masaki, Y. Ochi, *Mater. Sci. Eng. A* 417 (2006) 334–340, doi:[10.1016/j.msea.2005.11.017](https://doi.org/10.1016/j.msea.2005.11.017).
- [11] C.S. Montross, T. Wei, L. Ye, G. Clark, Y.W. Mai, *Int. J. Fatigue* 24 (2002) 1021–1036, doi:[10.1016/S0142-1123\(02\)00022-1](https://doi.org/10.1016/S0142-1123(02)00022-1).
- [12] C.S. Montross, T. Wei, L. Ye, G. Clark, Y.W. Mai, *Int. J. Fatigue* 24 (2002) 1021–1036, doi:[10.1016/S0142-1123\(02\)00022-1](https://doi.org/10.1016/S0142-1123(02)00022-1).
- [13] R. Fabbro, J. Fournier, P. Ballard, D. Devaux, J. Virmont, *J. Appl. Phys.* 68 (1990) 775–784, doi:[10.1063/1.346783](https://doi.org/10.1063/1.346783).
- [14] C.B. Schaffer, A. Brodeur, E. Mazur, *Measur. Sci. Technol.* 12 (2001) 1784 [stacks.iop.org/MST/12/1784](https://stacks.iop.org/MST/12/1784).
- [15] H. Nakano, S. Miyauti, N. Butani, T. Shibayanagi, M. Tsukamoto, N. Abe, *Laser Micro/Nanoeng.* 4 (2009) 35–38, doi:[10.2961/jlmm.2009.01.0007](https://doi.org/10.2961/jlmm.2009.01.0007).
- [16] T. Sano, T. Eimura, R. Kashiwabara, T. Matsuda, Y. Isshiki, A. Hirose, S. Tsutsumi, K. Arakawa, T. Hashimoto, K. Masaki, Y. Sano, *J. Laser Appl.* 29 (2017) 012005, doi:[10.2351/1.4967013](https://doi.org/10.2351/1.4967013).
- [17] D. Lee, E. Kannatey-Asibu, *J. Laser Appl.* 23 (2011) 022004, doi:[10.2351/1.3573370](https://doi.org/10.2351/1.3573370).
- [18] C.R. Phipps, T.P. Turner, R.F. Harrison, G.W. York, W.Z. Osborne, G.K. Anderson, X.F. Corlis, L.C. Haynes, H.S. Steele, K.C. Spicochi, T.R. King, *J. Appl. Phys.* 64 (1988) 1083–1096, doi:[10.1063/1.341867](https://doi.org/10.1063/1.341867).